



Pulse EPR Theory

Though Pulse EPR may seem a bit daunting in the beginning, there are a few simple principles that help you understand pulse EPR experiments. The first important principle to master is the rotating frame. Since Pulse EPR involves going between the time and frequency domains, we shall also discuss some of the important relations in Fourier theory. You will find that we will often use these simple principles throughout the coming chapters. The treatment is not mathematical, but intended to give you an intuitive understanding of the phenomena.

The Rotating Frame

The magnetization of your sample can often undergo very complicated motions. A useful technique, widely used in both CW and FT EPR and NMR, is to go to a rotating coordinate system, referred to as the rotating frame. From this alternative point of view, much of the mathematics is simplified and an intuitive understanding of the complicated motions can be gained.

A simple analogy for the rotating frame involves a carousel and two people trying to have a conversation. One person is riding on the carousel and the other person is standing still on the ground. Because the carousel is moving, the two people will be able to speak to each other only once per revolution and no meaningful conversation is possible. If, however, the person on the ground walks at the same speed as the carousel is rotating, the two people are next to each other continuously and they can carry on a meaningful conversation because they are stationary in the rotating frame.

The presentation is based on classical mechanics; the classical picture is often clearer and more productive than the quantum mechanical picture. Even though the phenomenon on a microscopic level is best described by quantum mechanics, we are measuring a bulk property of the sample, namely the magnetization, which is nicely described from a classical point of view.

Magnetization in the Lab Frame

In order to describe a physical phenomenon, we need to establish an axis system or reference frame. The reference frame which most people are familiar with is the lab frame which consists of three stationary mutually perpendicular axes. The lab frame in EPR is usually defined as in Figure 4.1. The magnetic field, B_0 is parallel to the z axis, the microwave magnetic field, B_1 , is parallel to the x axis, and the y axis is orthogonal to the x and z axes. All discussions of the electronic magnetization in this section will be described in this axis system.

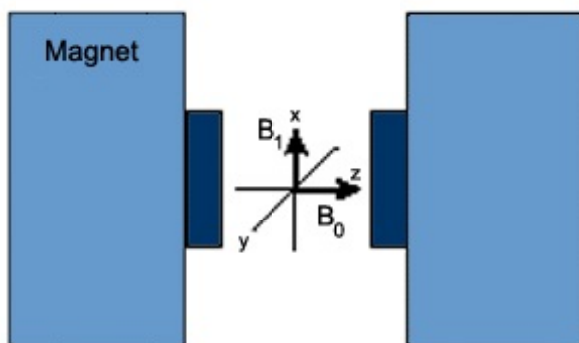


Figure 4.1: Definition of the lab axis system

When an electron spin is placed in a magnetic field, a torque is exerted on the electron spin, causing its magnetic moment to precess about the magnetic field just as a gyroscope precesses in a gravitational field. The angular frequency of the precession is commonly called the Larmor frequency and it is related to the magnetic field by

$$\omega_L = -\gamma B_0$$

equation 4.1

where ω_L is the Larmor frequency, γ is the constant of proportionality called the gyromagnetic ratio, and B_0 is the magnetic field. The sense of rotation and frequency depend on the value of γ and B_0 . A free electron has a $\gamma/2\pi$ value of approximately -2.8 MHz/Gauss, resulting in a Larmor frequency of about 9.75 GHz at a field of 3480 Gauss. The Larmor frequency corresponds to the EPR frequency at that magnetic field.

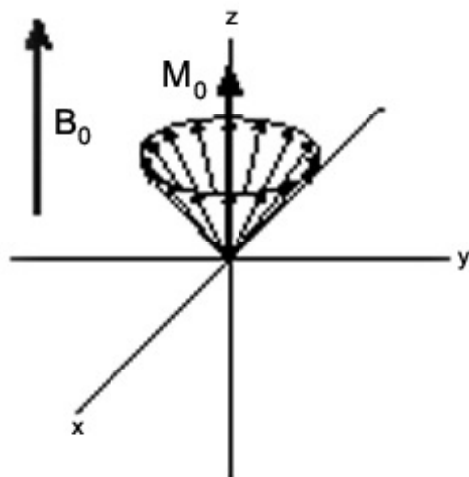


Figure 4.2: The Larmor precession and the resultant stationary magnetization

Let us consider a large number of electron spins in a magnetic field, B_0 , aligned along the z axis. (See Figure 4.2.) The electron spins are characterized by two quantum mechanical states, one with its magnetic moment parallel to B_0 and one antiparallel. The parallel state has lower energy and at thermal equilibrium, there is a surplus of electron spins in the parallel state according to the Boltzmann distribution. Therefore, there should be a net magnetization parallel to the z axis. (The magnetization is the vector sum of all the magnetic moments in the sample.) The electron spins are still precessing about the z axis, however their orientations are random in the x - y plane as there is no reason to prefer one direction over another. For a very large number of electron spins, the various transverse (*i.e.* in the x - y plane) components of the magnetic moments cancel each other out. The result is a stationary magnetization, M_0 , aligned along B_0 .

Magnetization in the Rotating Frame

EPR experiments are usually performed with a resonator using linearly polarized microwaves. The microwave resonator is designed to produce a microwave field, B_1 , perpendicular to the applied magnetic field, B_0 . In most cases, $|B_1| \ll |B_0|$.

Linearly polarized microwaves can be thought of as a magnetic field oscillating at the microwave frequency. (See the upper series of Figure 4.3.) An alternative way of looking at linearly polarized microwaves which is more useful when using the rotating frame is shown in the lower series of Figure 4.3. The sum of two magnetic fields rotating in opposite directions at the microwave frequency will produce a field equivalent to the linearly polarized microwaves. As we shall see, only one of the rotating components is important in describing the FT-EPR experiment.

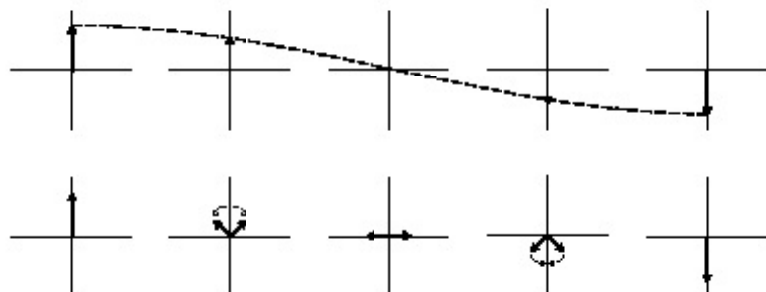


Figure 4.3: Linearly polarized microwaves represented as two circularly polarized components

Alas, the effect that B_1 has on the magnetization is very difficult to envision when everything is moving simultaneously as in the first picture in Figure 4.4. To avoid vertigo, we can observe what is happening from a rotating coordinate system in which we rotate synchronously with one of the rotating B_1 components. We shall assume that we are at resonance, *i.e.*

$$\omega_L = \omega_0$$

equation 4.2

where ω_0 is the microwave frequency. By rotating the coordinate system at an angular velocity of ω_0 , we can make one of the components of B_1 to appear

precessing at the Larmor frequency to appear stationary. Using Equation 4.1 and assuming the magnetization is not precessing in the rotating frame ($\omega = 0$), the field B_0 disappears in the rotating frame. In the rotating frame, we need only to concern ourselves with a stationary B_1 and M_0 .

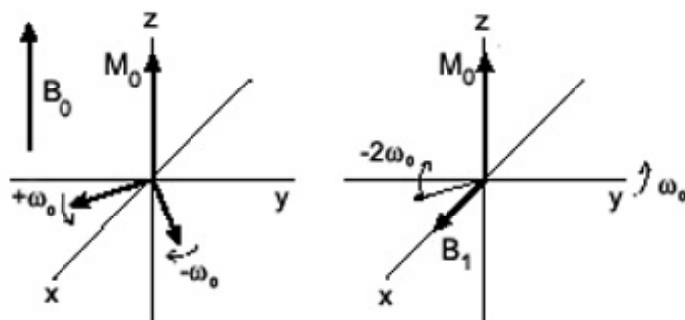


Figure 4.4: The microwave magnetic field in both reference frames

We have already looked at the interaction of a static magnetic field with the magnetization; the magnetization will precess about B_1 at a frequency,

$$\omega_1 = -\gamma B_1$$

equation 4.3

where ω_1 is also called the Rabi frequency. Let us assume that B_1 is parallel to the x axis. The magnetic field will rotate the magnetization about the +x axis as long as the microwaves are applied. (See Figure 4.5.)

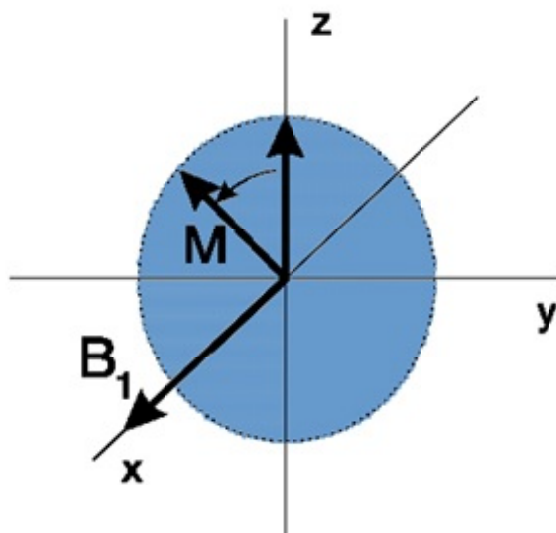


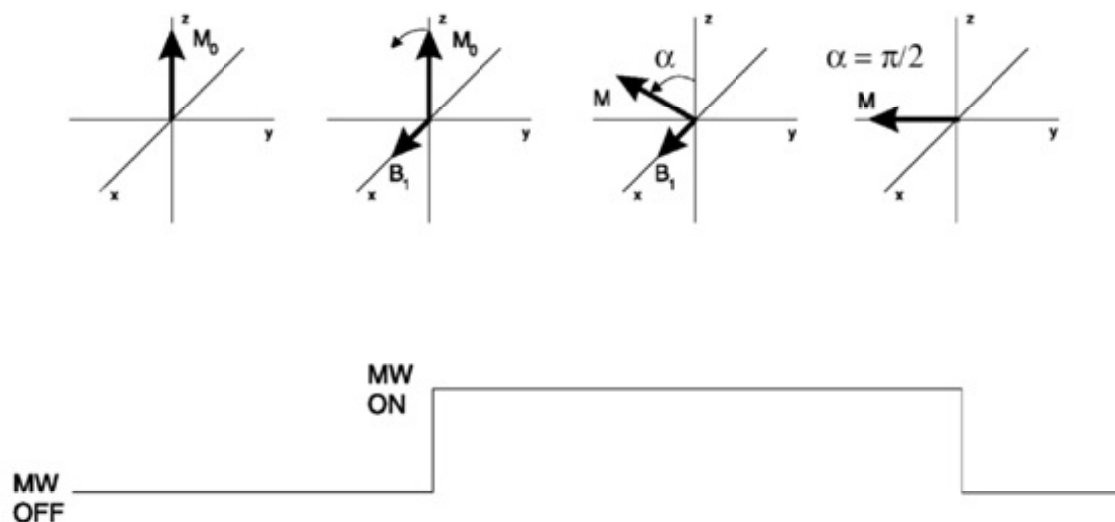
Figure 4.5: Rotating the magnetization

The angle by which M_0 is rotated, commonly called the tip angle, is equal to,

$$\alpha = -\gamma |B_1| t_p$$

equation 4.4

where t_p is the length of the pulse. Pulses are often labeled by their tip angle, i.e. a $\pi/2$ pulse corresponds to a rotation of M_0 by $\pi/2$. The most commonly used tip angles are $\pi/2$ and π (90 and 180 degrees). The tip angle is dependent on both the magnitude of B_1 and the length of the pulse. For example, a B_1 of 10 Gauss can often be obtained, resulting in a $\pi/2$ pulse length of approximately 9 ns. The effect of a $\pi/2$ pulse is shown in Figure 4.6; it results in a stationary magnetization along the -y axis. If we were to make the pulse twice as long, we would have a π pulse and the magnetization would be rotated to the -z axis.

Figure 4.6: The effect of a $\pi/2$ pulse

Because B_1 is parallel to $+x$ it is known as a $+x$ pulse. If we were to shift the phase of the microwaves by 90 degrees, B_1 would then lie along the $+y$ axis and the magnetization would end up along the $+x$ axis. Microwave pulses are therefore labeled not only by their tip angle but also by the axis to which B_1 is parallel.

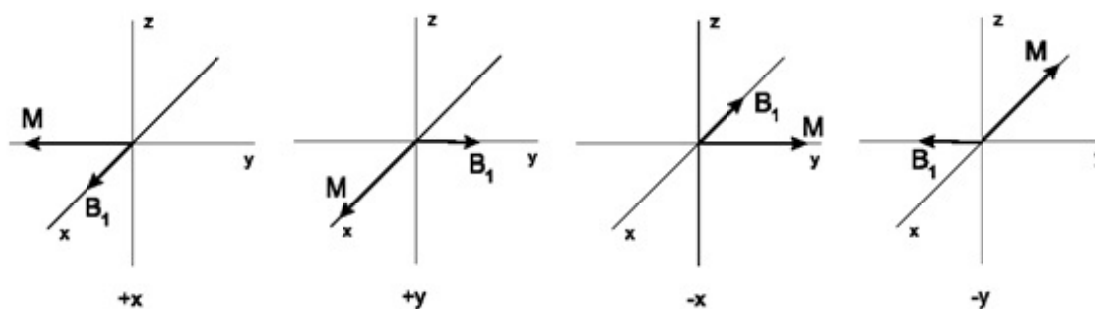


Figure 4.7: Four different pulse phases

Magnetization from Both Frames: The FID

In the introduction, it was mentioned that the sample emitted microwaves after the intense microwave pulse. How this happens is not completely clear if viewed from the rotating frame. If viewed from the lab frame, the picture is much clearer. The stationary magnetization along $-y$ then becomes a magnetization rotating in the x - y plane at the Larmor frequency. This generates currents and voltages in the resonator just like a generator. (See Figure 4.8 and Figure 4.9.) The signal will be maximized for the magnetization exactly in the x - y plane. This microwave signal generated in the resonator is called an FID (Free Induction Decay).

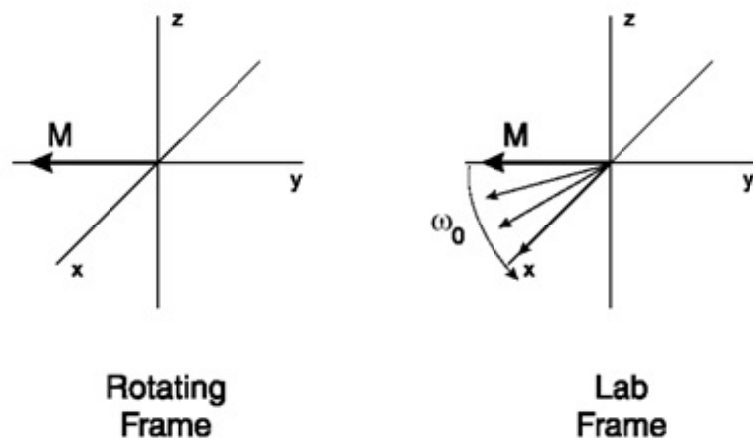


Figure 4.8: Generation of an FID

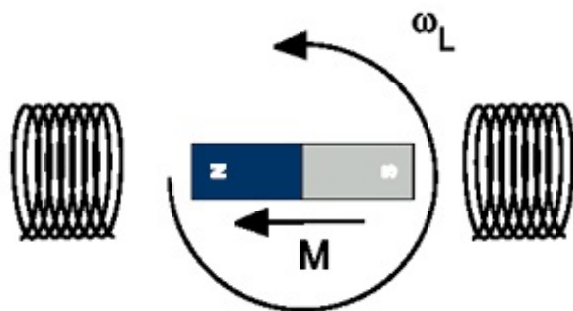


Figure 4.9: Rotation of the magnetization acting like a generator

Off Resonance Effects

So far we have been dealing with exact resonance conditions, *i.e.* the Larmor frequency is exactly equal to the microwave frequency. EPR spectra contain many different frequencies so not all parts of the EPR spectrum can be exactly on-resonance simultaneously. Therefore, we need to consider what happens to the magnetization when we are off-resonance.

First, we shall look at the rotating frame behavior of transverse magnetization having a frequency ω following a $\pi/2$ pulse. Initially the magnetization will be along the $-y$ axis, however, because ω is not equal to ω_0 , the magnetization will appear to rotate in the x - y plane. This means that the magnetization either is rotating faster or slower than the microwave magnetic field, B_1 . The rotation rate will be equal to the frequency difference:

$$\Delta\omega = \omega - \omega_0$$

equation 4.5

In the case of $\Delta\omega = 0$, the rotation rate is zero (*i.e.* stationary), which is precisely what we would expect for a system exactly on-resonance. If $\Delta\omega > 0$ the magnetization is gaining and will rotate in a counter-clockwise fashion. Conversely, if $\Delta\omega < 0$ the magnetization is lagging and will rotate in a clockwise fashion.

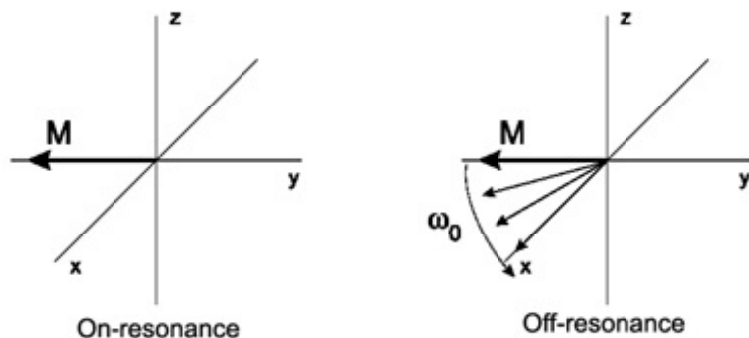


Figure 4.10: The magnetization in the rotating frame exactly on-resonance and $\Delta\omega$ off-resonance

This frequency behavior gives us a clue as to how the EPR spectrum is encoded in the FID. The individual frequency components of the EPR spectrum will appear as magnetization components rotating in the x-y plane at the corresponding frequency, $\Delta\omega$. If we could measure the transverse magnetization in the rotating frame, we could extract all the frequency components and hence reconstruct the EPR spectrum.

A second consequence of not being exactly on-resonance is that the microwave magnetic field B_1 actually tips the magnetization into the x-y plane differently because B_0 does not disappear when we are not on-resonance. We determined that B_0 disappears in the rotating frame when we were on-resonance because our magnetization is no longer precessing. When we are off-resonance, the magnetization is precessing at $\Delta\omega$ and therefore:

$$B_0 = \Delta\omega / -\gamma$$

equation 4.6

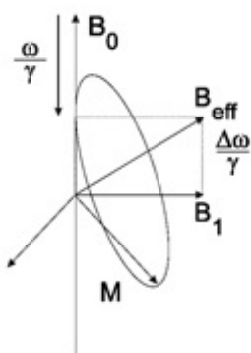


Figure 4.11: The effective microwave magnetic field in the rotating frame

Now the magnetization is not tipped by B_1 but by the vector sum of B_1 and B_0 , which is called B_{eff} or the effective magnetic field. The magnetization is then tipped about B_{eff} at the faster effective rate ω_{eff} :

$$\omega_{eff} = (\omega_1^2 + \Delta\omega^2)^{1/2}$$

equation 4.7

Another consequence is that we cannot tip the magnetization into the x-y plane as efficiently because B_{eff} does not lie in the x-y plane as B_1 does. The magnetization does not move in an arc as it does on-resonance, but instead its motion defines a cone. In fact, it can be shown that the magnetization that can be tipped in the x-y plane exhibits an oscillatory and decreasing behavior as $|\Delta\omega|$ gets larger:

$$M_y = M_0 * 1/(1 + (\Delta\omega/\omega_1)^2)^{1/2} * \sin((1 + (\Delta\omega/\omega_1)^2)^{1/2} * \pi/2)$$

equation 4.8

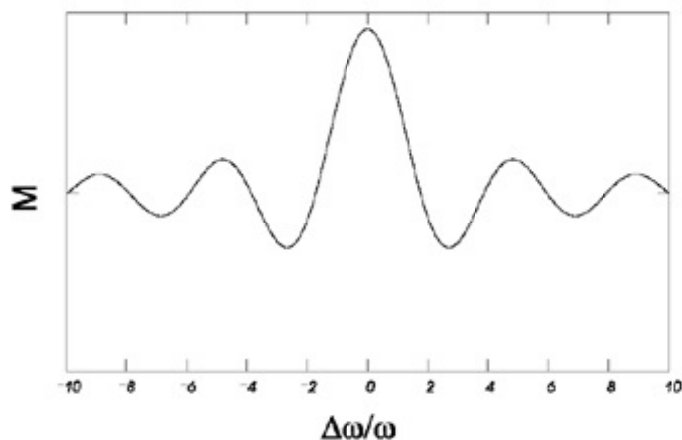


Figure 4.12: The transverse magnetization as a function of the offset after a $\pi/2$ pulse

One thing is evident from Figure 4.12, if we have a very broad EPR spectrum ($\Delta\omega > \omega_1$), we will not be able to tip all the magnetization into the x-y plane to create an FID. This is why it is important to maximize ω_1 (or equivalently to minimize the $\pi/2$ pulse length) for broad EPR signals. As B_1 gets larger (and the pulse lengths get shorter), we can successfully detect more of our EPR spectrum. (See Figure 4.13.)

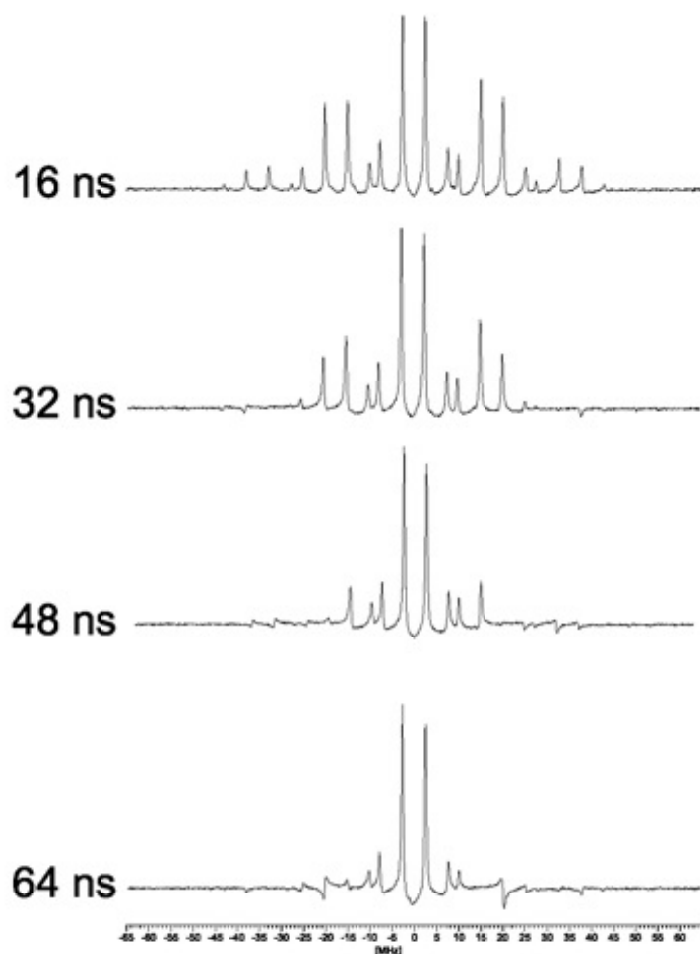


Figure 4.13: The effect of pulse length on an FT-EPR spectrum of the perinaphthényl radical

Relaxation Times

So far our description is a bit unrealistic because when we tipped the magnetization into the x-y plane, it remained there with the same magnitude. Because the electron spins interact with their surroundings, the magnetization in the x-y plane will decay away and eventually the magnetization will once more return to alignment with the z axis. This process is called relaxation and is characterized by two constants, T_1 and T_2 . The spin lattice relaxation time, T_1 , describes how quickly the magnetization returns to alignment with the z axis. The transverse relaxation time, T_2 describes how quickly the magnetization in the x-y plane (i.e. transverse magnetization) disappears.

states is equal to:

$$n_{\text{anti-parallel}} / n_{\text{parallel}} = e^{-\Delta E/kT}$$

equation 4.9

where n represents the populations of the two states, ΔE is the energy difference between the two states, k is Boltzmann's constant and T is the temperature. The magnetization that we have been discussing so far is actually the vector sum of all the magnetic moments in the sample. Since the moments can only be either parallel or anti-parallel, the magnetization is simply proportional to the difference, $n_{\text{parallel}} - n_{\text{anti-parallel}}$ and will be aligned along the z axis. To get an idea of the size of the population differences, if we are working at X-band (~ 9.8 GHz) at room temperature (300 K) with a sample with 10,000 spins, on average 5,004 spins would be parallel and 4996 spins would be anti-parallel resulting in a population difference of only 8. At room temperature and X-band, we are dealing with a small population difference between the two states. When we apply a $\pi/2$ pulse to our sample, we no longer have thermal equilibrium. How does this happen? When B_1 rotates the magnetization into the x - y plane, the magnetization along the z axis goes to zero, i.e. the population difference goes to zero. (See Figure 4.14.) If we were to use Equation 4.9 to estimate the temperature of our spins, we would obtain $T = \text{infinity}$. Our spin system is obviously not in thermal equilibrium and through its interactions with the surroundings, it will eventually return to thermal equilibrium. This process is called spin-lattice relaxation.

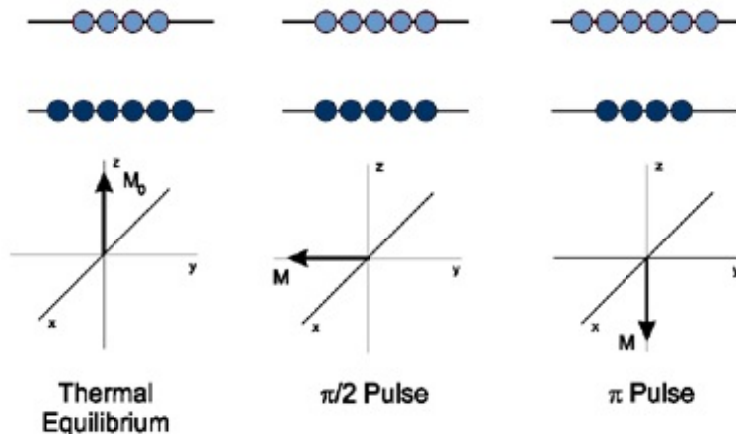


Figure 4.14: Populations before and after $\pi/2$ and π pulses

We could go even one step further and apply a π pulse. This will actually rotate the magnetization anti-parallel to the z -axis, corresponding to more magnetic moments aligned along the $-z$ axis. (This is why a π pulse is often referred to an inversion pulse.) If we use Equation 4.9, we actually calculate a negative temperature.

The rate constant at which M_z recovers to thermal equilibrium is T_1 , the spin-lattice relaxation time. The magnetization will exhibit the following behavior after a $\pi/2$ pulse:

$$M_z(t) = M_0 * (1 - e^{-(t/T_1)})$$

equation 4.10

or after a π pulse:

$$M_z(t) = M_0 * (1 - 2 * e^{-(t/T_1)})$$

equation 4.11

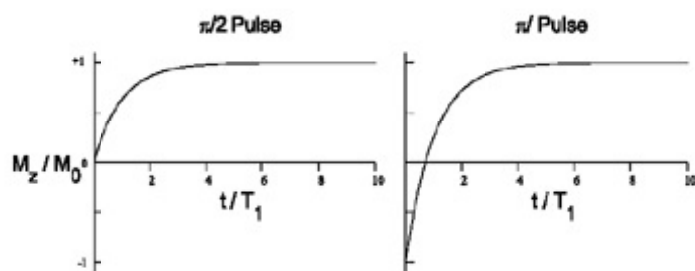


Figure 4.15: Recovery of the magnetization after a microwave pulse

In order to extract our signals from the noise, we must signal average the FID by repeating the experiment as quickly as possible and adding up the individual signals. What does "as quickly as possible" mean? We must wait until the magnetization along the z axis has recovered, because if there is no z magnetization, you cannot tip it into the x - y plane to create a FID. The first FID will be maximum and the following FIDs will eventually approach a limit value that is smaller than the initial value. (See Figure 4.16.)

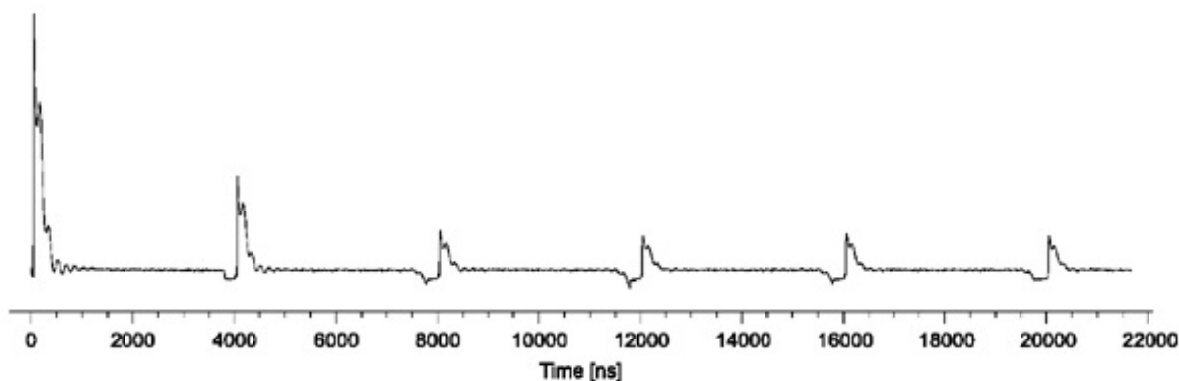


Figure 4.16: Repeating an FID experiment too quickly

The limit value as a function of T_1 and SRT (the Shot Repetition Time, which is the time between individual experiments) is equal to:

$$M_z(\text{SRT}) = M_0 * (1 - e^{-(\text{SRT}/T_1)})$$

equation 4.12

One important fact is that if $\text{SRT} = 5 \times T_1$, 99% of the magnetization will have recovered before the next experiment.

Transverse Relaxation Time

The transverse relaxation time corresponds to the time required for the magnetization to decay in the x-y plane. There are two main contributions to this process and they are related to different broadening mechanisms: homogeneous and inhomogeneous broadening.

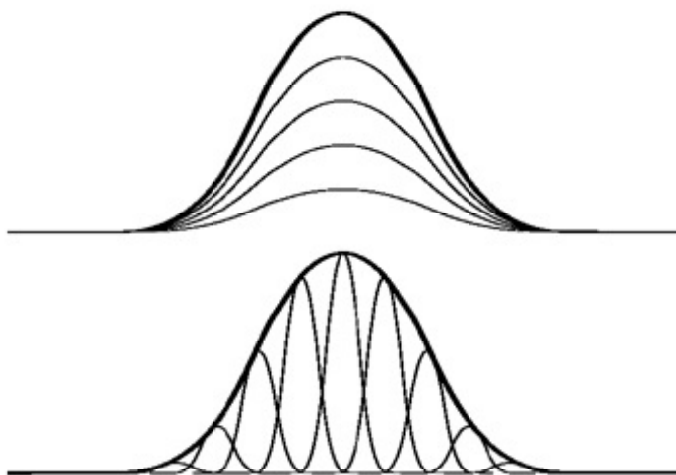


Figure 4.17: a) Homogeneous broadening. The lineshape is determined by the relaxation times and therefore Lorentzian lineshapes are a common result. (See Equation 4.13 and Figure 4.21) The EPR spectrum is the sum of a large number of lines each having the same Larmor frequency and linewidth.

b) Inhomogeneous broadening. The lineshape is determined by unresolved couplings because the EPR spectrum is the sum of a large number of narrower individual homogeneously broadened lines that are each shifted in frequency with respect to each other. Gaussian lineshapes are a common result.

In an inhomogeneously broadened spectrum, the spectrum is broadened because the spins experience different magnetic fields. These different fields may arise from unresolved hyperfine structure in which there are so many overlapping lines that the spectrum appears as one broad signal. (See Figure 4.17.) Typically this type of broadening results in a Gaussian lineshape, which we shall discuss in the next section.

This distribution of local fields gives us a large number of spin-packets characterized by a distribution of $\Delta\omega$ in the rotating frame. As shown in Figure 4.10, the magnetization of an individual spin-packet will rotate if $\Delta\omega$ not equal to 0 and the larger $\Delta\omega$ is, the faster it rotates. If we sum up all the components of the individual spin-packets, we see that many components cancel each other out and decrease the transverse magnetization. (See Figure 4.18) The shape of this transverse

the decay is called T_2^* . (T two star.)

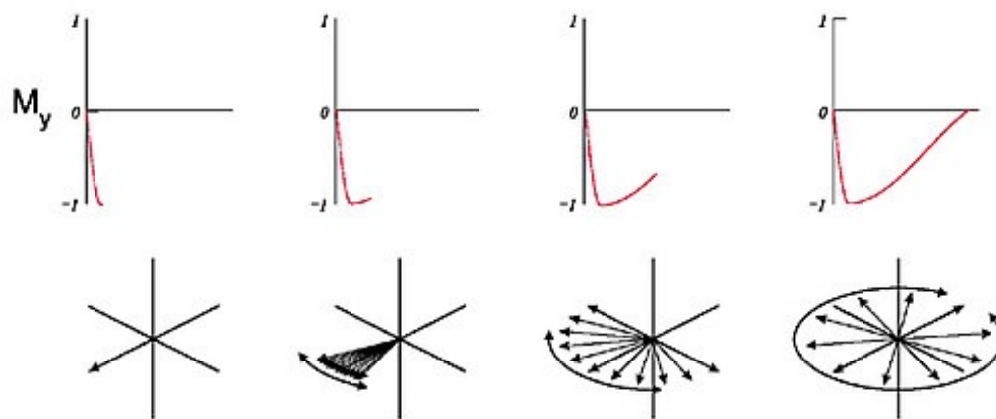


Figure 4.18: Fanning out of the transverse magnetization and the decrease of the transverse magnetization

In Figure 4.17, each of the individual spectra (or spin-packets) which comprise the inhomogeneously broadened line are homogeneously broadened. In a homogeneously broadened spectrum, all the spins experience the same magnetic field. The spins interact with each other, resulting in mutual and random spin flip-flops. Molecular motion can also contribute to this relaxation. These random fluctuations contribute to a faster fanning out of the magnetization. This broadening mechanism results in Lorentzian lineshapes which we shall discuss in the next section. The decay of the transverse magnetization (FID) from this mechanism is in general exponential:

$$M_y = e^{-(t/T_2)}$$

equation 4.13

where T_2 is often called the spin-spin relaxation time.

A Few Fourier Facts

So far, all our discussions have been very geometric. It was mentioned that the information about the frequency spectrum was somehow encoded in the transverse magnetization in the rotating frame. One means of reconstructing the frequency spectrum is to study the time behavior of the transverse magnetization. (See Figure 4.19.) The component of the transverse magnetization along the $-y$ axis will vary as:

$$M_y = M \cos \Delta\omega t$$

equation 4.14

where $\Delta\omega$ is the frequency offset $\omega - \omega_0$ and t is the time after the microwave pulse. The component along $+x$ will vary as:

$$M_x = M \sin \Delta\omega t$$

equation 4.15

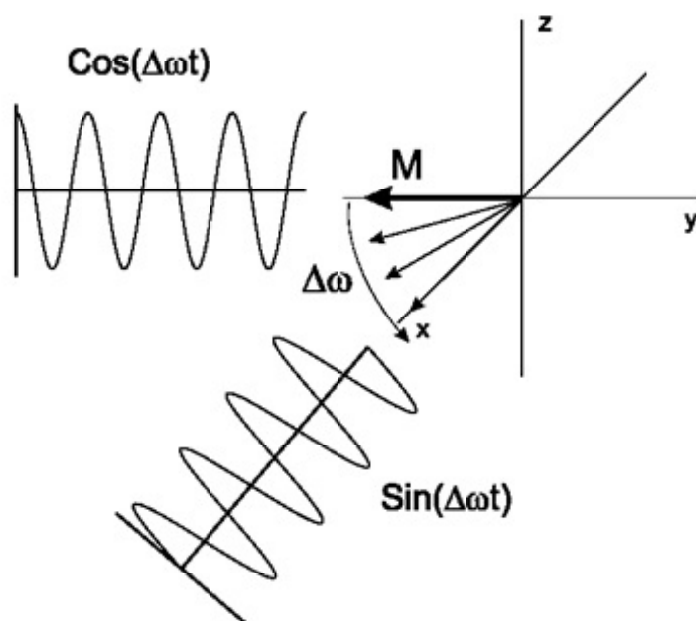


Figure 4.19: Time behavior of the transverse magnetization

A common mathematical convenience is to treat these two components as the real and imaginary components of a complex quantity:

where

$$e^{i\phi} = \cos \phi + i \sin \phi$$

equation 4.17

and

$$i = (-1)^{1/2}$$

equation 4.18

The transverse magnetization can then be represented by a vector in the x-y plane. It has both a magnitude M and a direction represented by the phase angle ϕ .

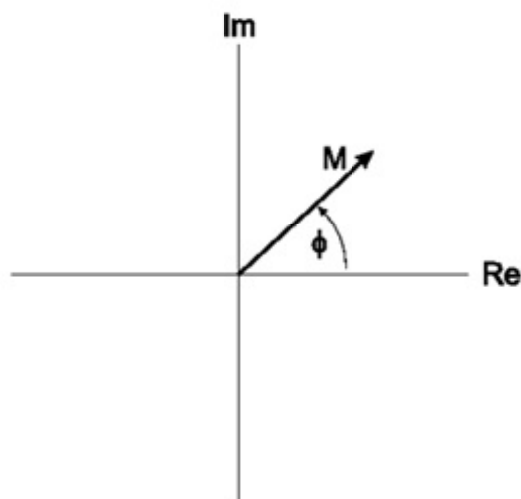


Figure 4.20: Representation of the transverse magnetization as a complex quantity

The reason why we go to this representation is because we can now use Fourier theory. Fourier theory relates a time domain signal with its frequency domain representation via the Fourier transform. This transform is the means by which we extract our EPR spectrum from the FID.

It is not the purpose of this primer to make you an expert in the arcane secrets of Fourier theory. A few theorems and identities can offer you an intuitive and visual understanding of many things you will encounter in pulse EPR.

The Fourier Transform

We can represent a function either in the time domain or the frequency domain. It is the Fourier transform which converts between the two representations. The Fourier transform is defined by the expression:

$$F(\omega) = \int f(t) e^{-i\omega t} dt$$

equation 4.19

There is also an inverse Fourier transform:

$$F(t) = 1/(2\pi) \int F(\omega) e^{i\omega t} d\omega$$

equation 4.20

Fourier Transform Pairs

We do not necessarily have to understand these equations in great detail. Any functions related by Equation 4.19 and Equation 4.20 form what is called a Fourier transform pair. The pairs that we shall encounter frequently are shown in Figure 4.21. The important points to learn are:

- Though a function may be purely real, it will in general have a complex Fourier transform.
- Even functions ($f(-t) = f(t)$ also called symmetric) have a purely real Fourier transform. (See Figure 4.21 a.)
- Odd functions ($f(-t) = -f(t)$ also called anti-symmetric) have a purely imaginary Fourier transform. (See Figure 4.21 b.)
- An exponential decay in the time domain is a lorentzian in the frequency domain. (See Figure 4.21 c.)
- A gaussian decay in the time domain is a gaussian in the frequency domain. (See Figure 4.21 d.)
- Quickly decaying signals in the time domain are broad in the frequency domain.
- Slowly decaying signals in the time domain are narrow in the frequency domain.
- These pairs are reciprocal, i.e. a lorentzian in the time domain results in a decaying exponential in the frequency domain.

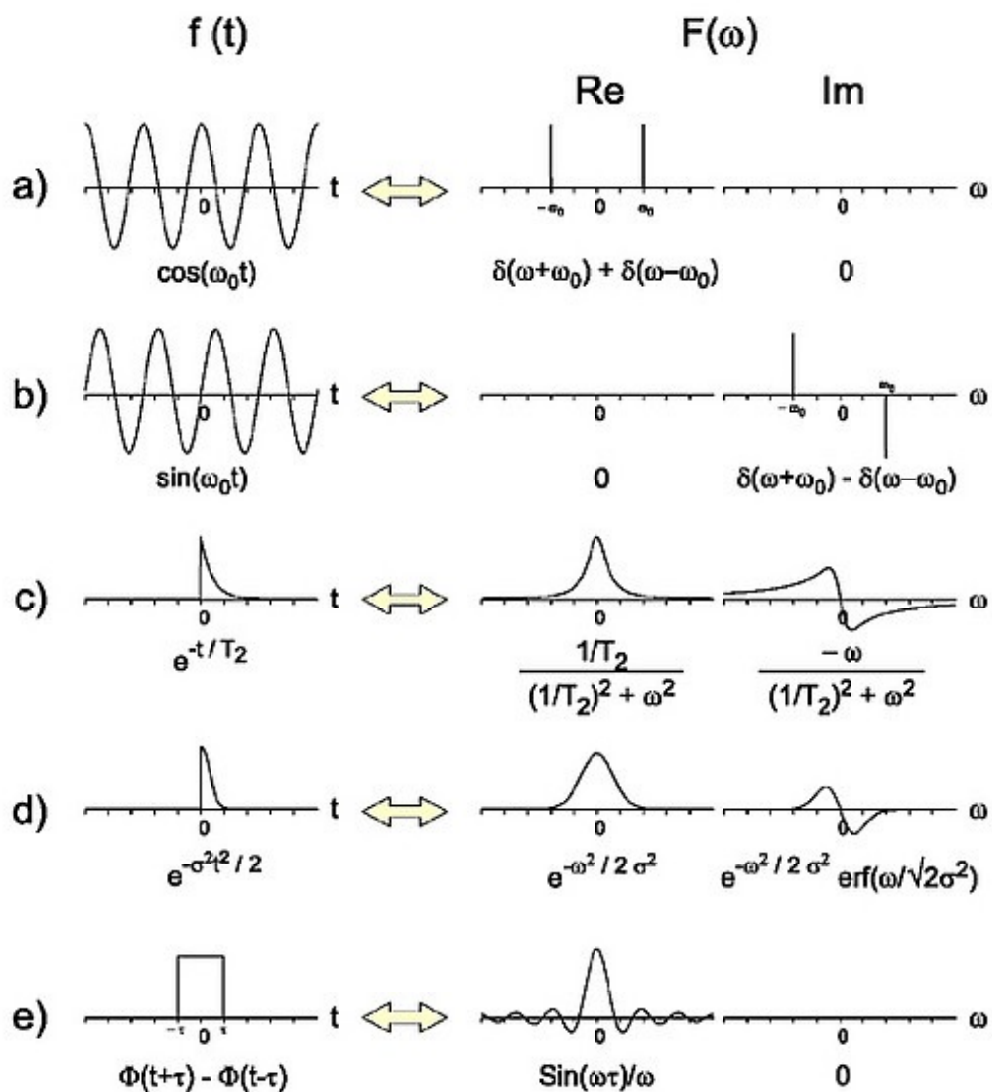


Figure 4.21: Useful Fourier transform pairs (for simplicity, $F(\omega)$ normalization constants are omitted)

Fourier Transform Properties

One important property that we shall need is that the Fourier transform of the sum of two functions is equal to the sum of the Fourier transforms:

$$f(t) + g(t) \Leftrightarrow F(\omega) + G(\omega)$$

equation 4.21

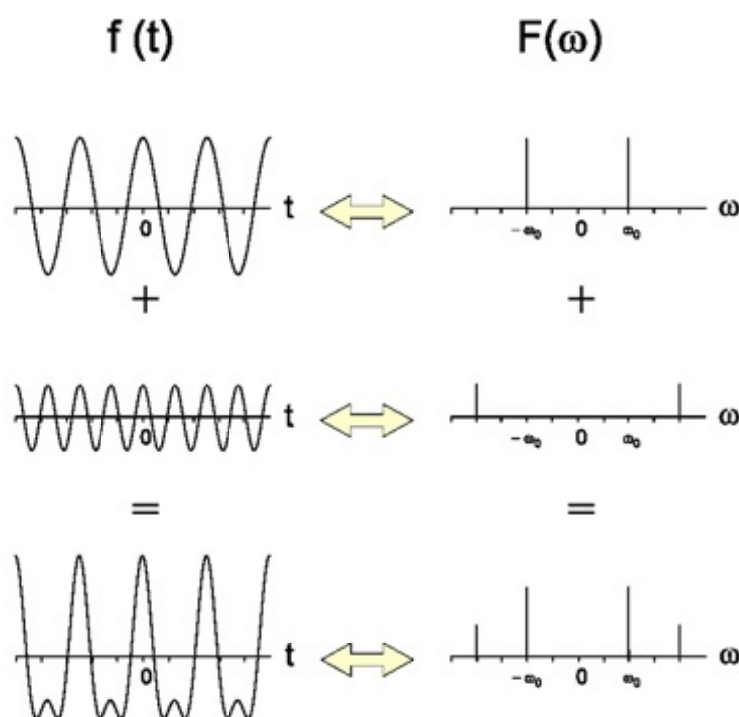


Figure 4.22: The addition property of the Fourier transform

Another important property is how the frequency domain signal changes as we time shift (delay or advance the signal in time) the time domain signal or how the time domain signal changes if we frequency shift the frequency domain signal. After a bit of math, we obtain the following Fourier transform pairs:

$$f(t - \Delta t) \Leftrightarrow F(\omega) * e^{-i\omega\Delta t}$$

equation 4.22

$$f(t) * e^{i\Delta\omega t} \Leftrightarrow F(\omega - \Delta\omega)$$

equation 4.23

When time shifting, we obtain the original frequency domain signal with a frequency dependent phase shift. As we can see from Figure 4.23, the phase shift transfers some of the real signal to the imaginary and vice versa. This effect leads to the well known linear phase distortion (and correction) in Fourier transform spectroscopy. We start off in Figure 4.23 with a purely real signal (remember that a symmetric signal has a purely real Fourier transform) and after the time delay we obtain an oscillating mixture of real and imaginary components. Because of the reciprocal nature of Fourier transform pairs, similar behavior in the time domain signal is observed when the frequency is shifted in the frequency domain signal.

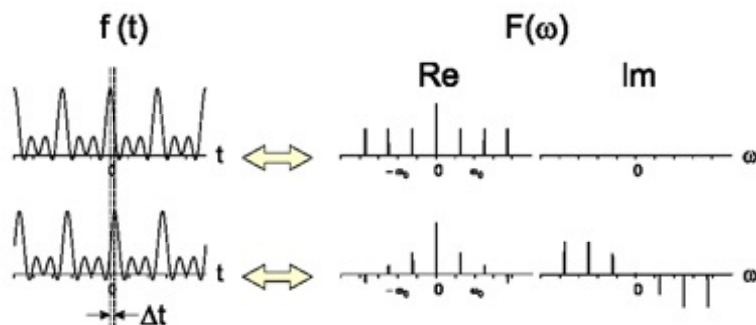


Figure 4.23: The time shift properties of the Fourier transform

The Convolution Theorem

The convolution integral appears frequently in a number of scientific disciplines. The convolution of two functions is defined as:

$$f(t) * g(t) = \int f(\tau)g(t-\tau)d\tau$$

equation 4.24

It can also be shown that $f(t) * g(t) = g(t) * f(t)$.

It is difficult to envision exactly what the convolution is doing, but it can be interpreted loosely as a running average of the two functions. In the limit of a Dirac delta function (*i.e.* a spike), the convolution can be graphically represented as in Figure 4.24. We are placing a copy of our function at each of the spikes.



Figure 4.24: The convolution of two functions

The convolution theorem states that the Fourier transform of the convolution of two functions is equal to the product of the Fourier transforms of the individual functions. We now have two new Fourier transform pairs:

$$f(t) * g(t) \Leftrightarrow F(\omega) G(\omega)$$

equation 4.25

$$F(\omega) * G(\omega) \Leftrightarrow f(t) g(t)$$

equation 4.26

So the convolution theorem gives us an easy way to calculate a convolution integral if we know the individual Fourier transforms. More importantly, it offers us a powerful means of envisioning time signals in the frequency domain and vice versa.

A Practical Example

Now its time to start applying what we have learned in the previous sections to a concrete problem, predicting what a time domain signal (*e.g.* a FID) looks like if we are given a frequency domain signal (*e.g.* an EPR spectrum). As an example, we consider a three line EPR spectrum such as a nitroxide. (See Figure 4.25.) We assume that the magnetic field is set so that the center line is on-resonance, the lines are lorentzian, and the splitting is equal to A. Remember that in an FT experiment we are detecting both the absorption (real) and dispersion (imaginary) signals.

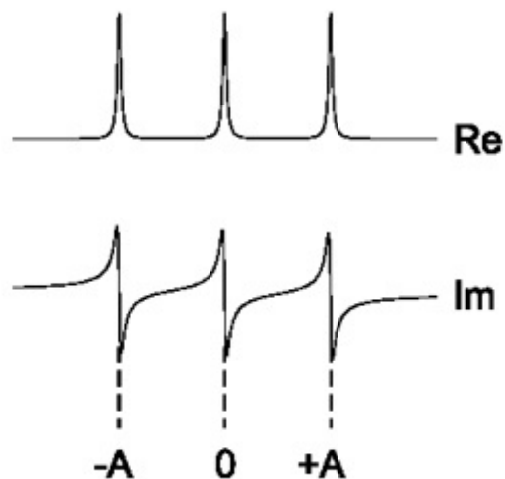


Figure 4.25: A three line EPR spectrum with both absorptive and dispersive components

The first thing to notice is that we can deconvolute the spectrum into a stick spectrum and a Lorentzian function.

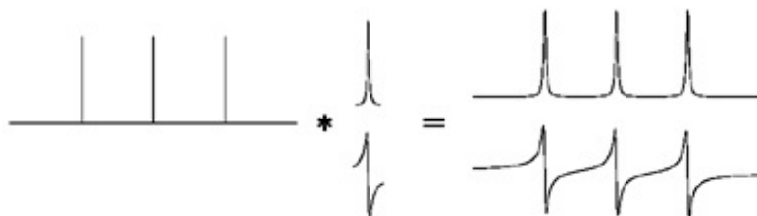


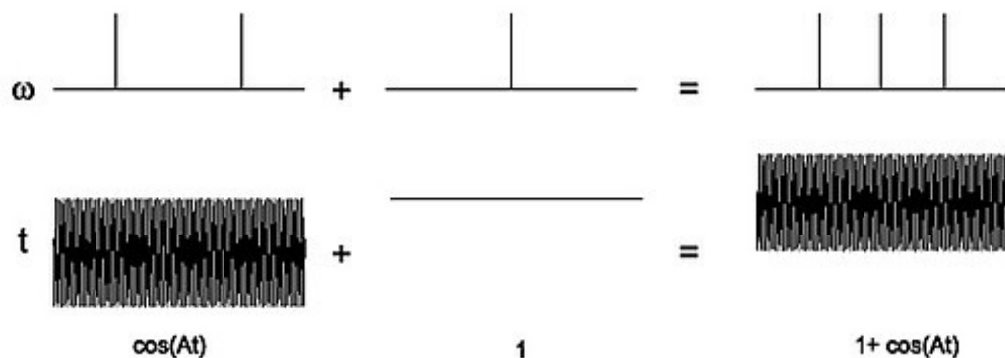
Figure 4.26: Deconvoluting an EPR spectrum into a stick spectrum and a Lorentzian function

We know from the convolution theorem that the time domain signal is simply the product of the two transformed functions. (See Equation 4.26.) We already know the Fourier transform for a Lorentzian:

$$e^{-t/T_2}$$

equation 4.27

Next we have to calculate the Fourier transform of the three line stick spectrum. One thing that helps is that this signal is symmetric, yielding a purely real time domain signal. Using the additive properties of Fourier transforms, we express the three line stick spectrum as the sum of two signals with known Fourier transforms. Adding the two time domain signals gives us the Fourier transform of the stick spectrum.



Multiplying the two time domain functions gives us the result in Figure 4.28. This is the FID of the three line EPR spectrum.

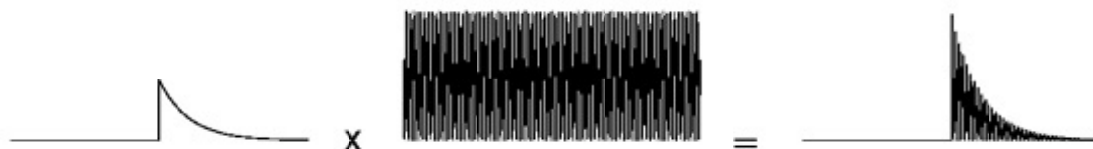


Figure 4.28: FID of a three line EPR spectrum

The next three figures are examples of what happens to the FID when the EPR signal changes.

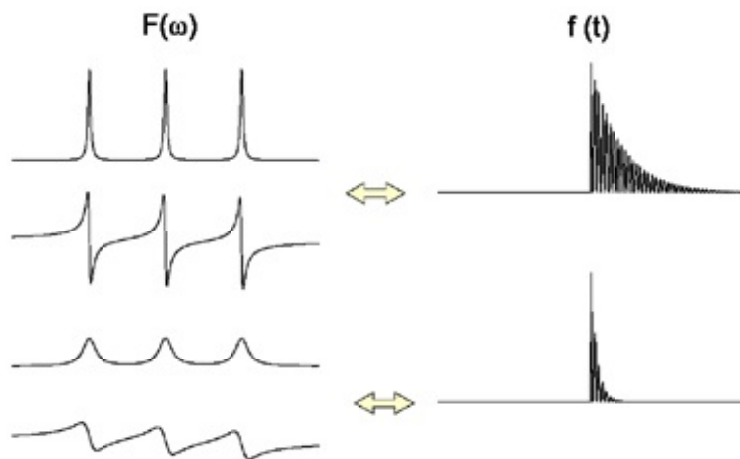


Figure 4.29: The effect of linewidth

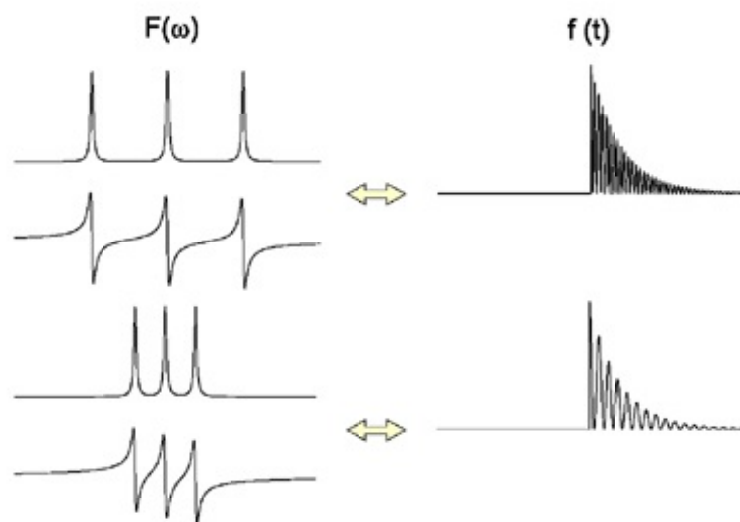


Figure 4.30: The effect of line splittings

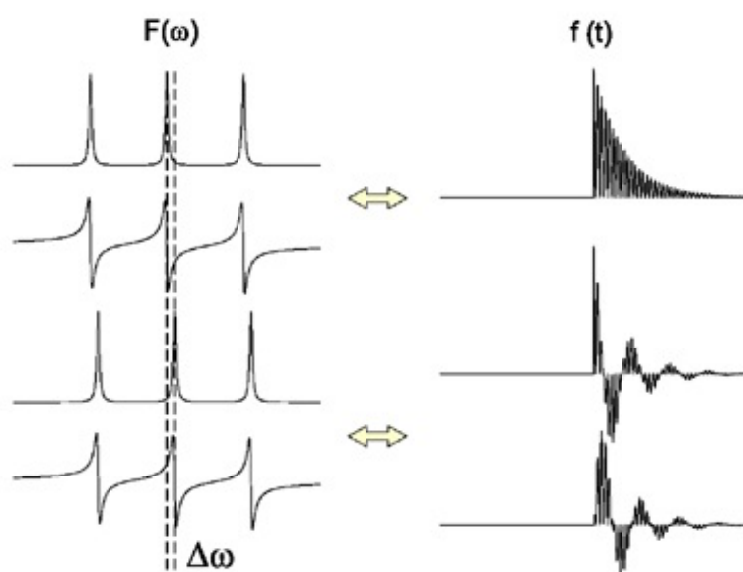


Figure 4.31: The effect of a frequency shift

These practical examples demonstrate that if we make use of the Fourier transform pairs, properties, and convolution theorem, we can easily envision how signals appear in both time and frequency domains. We do not have to perform any complicated mathematical operations to Fourier transform our signals. We can visually estimate the appearance of signals in both the time and frequency domains. Even though this intuitive ability is not mandatory, it comes in very handy later on when adjusting parameters and processing data.

Field Sweep vs. Frequency Sweep

A little bit of care is required when comparing conventional field swept spectra and frequency spectra obtained by FT-EPR. The field and frequency axes run in opposite directions. Here are two spectra of the same sample. The upper spectrum is a frequency spectrum acquired by Fourier transforming the echo (To be discussed in the next section.). The lower spectrum was acquired in a conventional field swept experiment.



Figure 4.32: Field sweeps and frequency spectrum are mirror images of each other

In Figure 4.33 we see the Larmor frequencies when the field is set so the center line is on-resonance. The higher field line actually has a lower (negative) Larmor frequency than the center line. We need to apply more magnetic field to increase its Larmor frequency so that it would be on-resonance with the microwaves. The lower field line has a higher Larmor frequency.

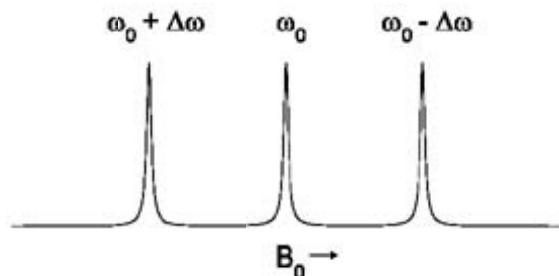


Figure 4.33: Larmor frequencies when B_0 is set for resonance on the center line

Multiple Pulse = Echoes

As we have seen in the previous sections, one microwave pulse produces a signal that decays away (FID). If our EPR spectrum is inhomogeneously broadened, we can recover this disappeared signal with another microwave pulse to produce a Hahn echo.

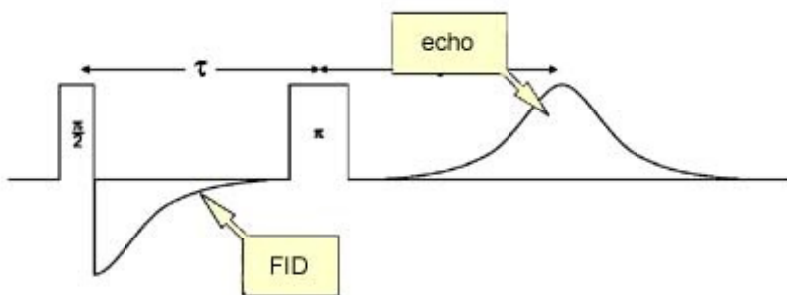


Figure 4.34: A Hahn echo

Echoes are important in EPR because FIDs of very broad spectra decay away very quickly. We shall see in the second part of this chapter that we cannot detect signals during an approximately 80 ns period after the microwave pulse. This period of time is called the *deadtime*. If the FID is very short, it will disappear before the deadtime ends. If we make τ long enough, we can ensure that the echo appears after the deadtime.

How Echoes Occur

How does the echo bring back our signal? The decay of the FID is due to the different frequencies in the EPR spectrum causing the magnetization to fan out in the x-y plane of the rotating frame. When we apply the π pulse, we flip the magnetization about the x axis. The magnetization still rotates in the same direction and speed. This almost has the effect of running the FID backwards in time. The higher frequency spin packets will have traveled further than the lower frequency spin packets after the first pulse. However, because the higher frequency spin packets are rotating more quickly, they will eventually catch up with the lower frequency spin packets along the +y axis after the second pulse. (See Figure 4.35.)

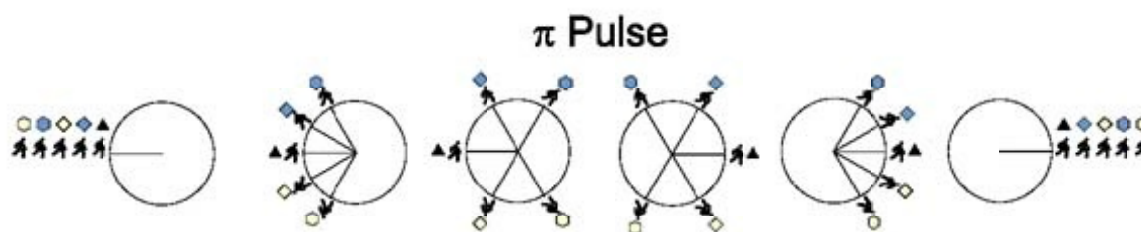


Figure 4.35: Refocusing of the magnetization during an echo

After all the spin packets bunch up, they will dephase again just like a FID. So one way to think about a spin echo is a time reversed FID followed by a normal FID. Therefore, if we Fourier transform the second half of the FID, we obtain the EPR spectrum.

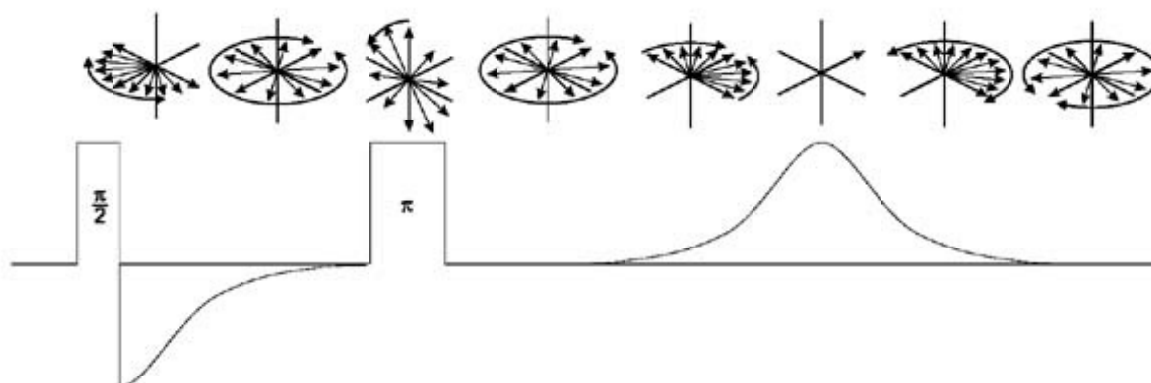


Figure 4.36: Magnetization behavior during an echo experiment

In all we have said so far, we should be able to make τ , the pulse separation, very long and still obtain an echo. Transverse relaxation leads to an exponential decay in echo height:

$$\text{echo height}(\tau) \propto e^{-2\tau/T_M}$$

equation 4.28

where T_M , the phase memory time, is the decay constant. Many processes contribute to T_M such as T_2 (spin-spin relaxation), as well as spectral, spin, and instantaneous diffusion.

Notice the factor of two in Equation 4.28 which is not in the expression for the FID. This is because dephasing starts after the first pulse and the echo occurs at 2 after the first pulse. So by studying the echo decay as we increase τ , we can measure T_M .

Spectral diffusion often is a large contributor to T_M . Nuclear spin flip-flops, molecular motion, and molecular rotation can cause spin packets to suddenly change their frequency. A faster spin packet far from the +y axis will suddenly become a slower spin packet without the needed speed to catch up with the other spin packets in their race to refocus. Therefore, we are not refocusing all the magnetization. In Figure 4.37 we see that after the runner marked with an asterisk has a shifted frequency, we only get four of the five runners lining up to refocus.

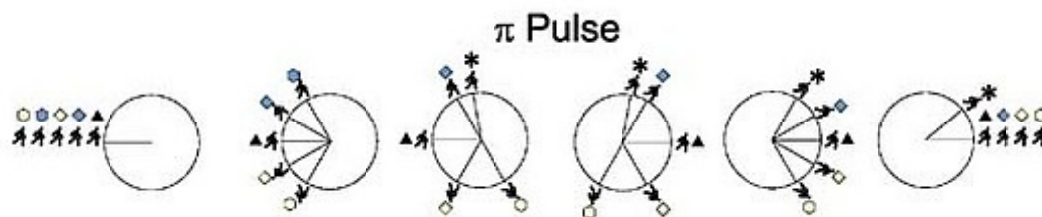
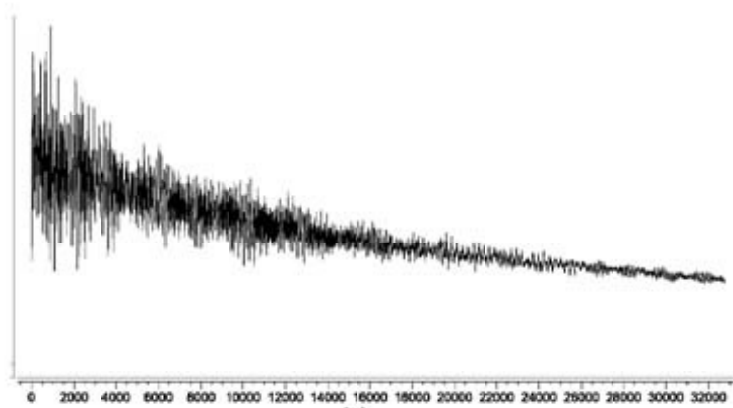


Figure 4.37: Dephasing due to a sudden frequency shift (the asterisk marks the runner whose frequency has suddenly become less)

ESEEM

A very important class of echo experiments is ESEEM (Electron Spin Echo Envelope Modulation). The electron spins interact with the nuclei in their vicinity and this interaction causes a periodic oscillation in the echo height superimposed on the normal echo decay. The modulation or oscillation is caused by periodic dephasing by the nuclei. If we subtract the decay of the spin echo and Fourier transform the oscillations, we obtain the splittings due to the nuclei. Armed with this information, you can identify nearby nuclei and their distances from the electron spin and shed light on the local environment of the radical or metal ion.



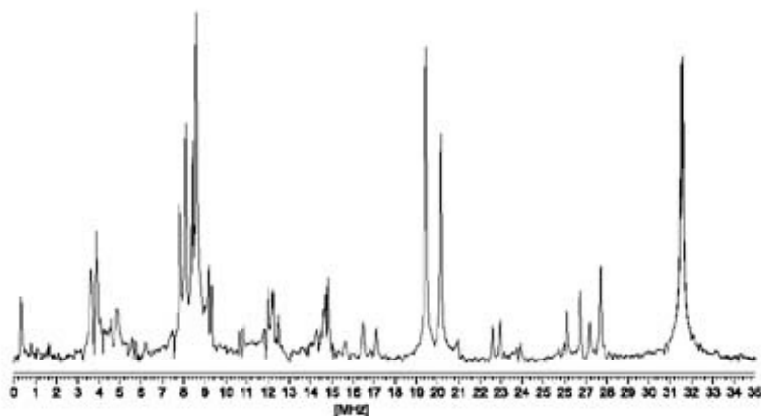


Figure 4.39: The Fourier transform of the ESEEM showing proton couplings

Stimulated Echoes

Hahn or two pulse echoes are not the only echoes to occur. If we apply three $\pi/2$ pulses we obtain five echoes. Three of the echoes are simply two pulse echoes produced by the three pulses. The stimulated and refocused echoes only occur when you have applied more than two pulses.

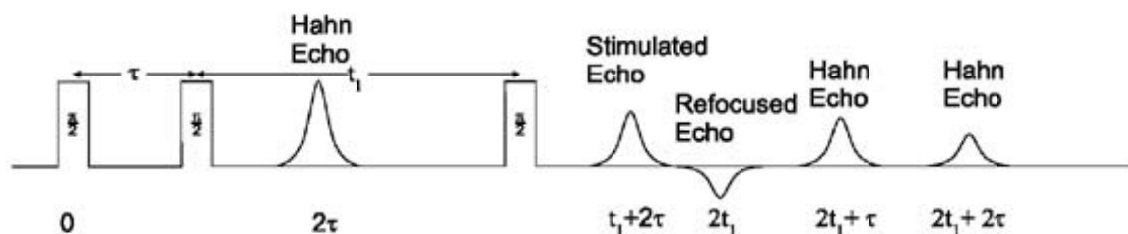


Figure 4.40: Echoes and timing in a three pulse experiment

The stimulated echo is particularly important because it also exhibits ESEEM effects when t_1 is varied. A Hahn echo decays with a time constant of $T_M/2$ whereas the stimulated echo decays with a time constant of approximately T_1 . (Spin and spectral diffusion contributions causes the stimulated echo to decay somewhat faster than T_1 .) T_M is often much shorter than T_1 , so the ESEEM decays more slowly in a stimulated echo than in a Hahn echo experiment. Therefore, a three pulse ESEEM experiment usually gives superior resolution than a two pulse ESEEM experiment.

Pulse Lengths and Bandwidths

In Pulse EPR spectroscopy, we often can excite only a small portion of our EPR spectrum. This fact simplifies things when performing echo experiments. First, if we have a very broad EPR spectrum, within the range of our excitation of the spectrum it looks almost flat and therefore approximately symmetric. As a consequence, our echo will be purely real with no imaginary component. Second, the echo width is approximately equal to the pulse width.

Quite often it is more convenient to use two equal length pulses instead of the traditional $\pi/2 - \pi$ pulse sequence. The reason for doing this is the π pulse is twice as long as the $\pi/2$ pulse and therefore will limit the amount of the EPR spectrum we can excite. (See Figure 4.21e.) With a bit of calculus, it can be shown that the maximum echo height for two equal length pulses is achieved with two $2\pi/3$ (120°) pulses. (See Figure 4.41.) The narrower $2\pi/3$ pulses excite a broader portion of our spectrum than the π pulse can.

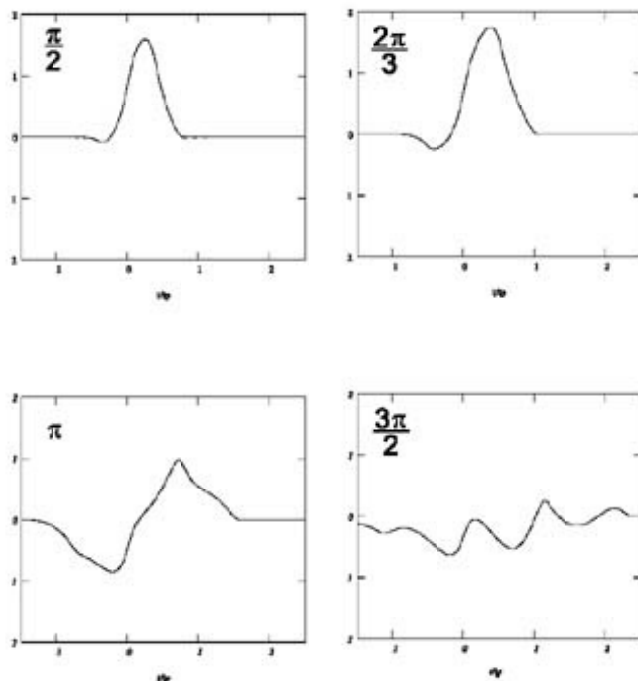


Figure 4.41: Simulated echo shapes for different tip angles.

Sometimes both hard (short) and soft (long) pulses are combined together in one experiment. For example, to perform a Davies pulse ENDOR experiment, you use a soft π pulse to burn a narrow hole in the EPR spectrum (See Figure 4.42.) and two narrow pulses to detect it.

The resulting echo can be a bit puzzling at first glance. It is actually the sum of two echoes: one is a narrow positive going echo from the broad EPR spectrum and the other is a broad negative going echo from the narrow hole. In order to adjust the π pulse, the microwave power is varied until the area of the broad negative going echo is as negative as possible.

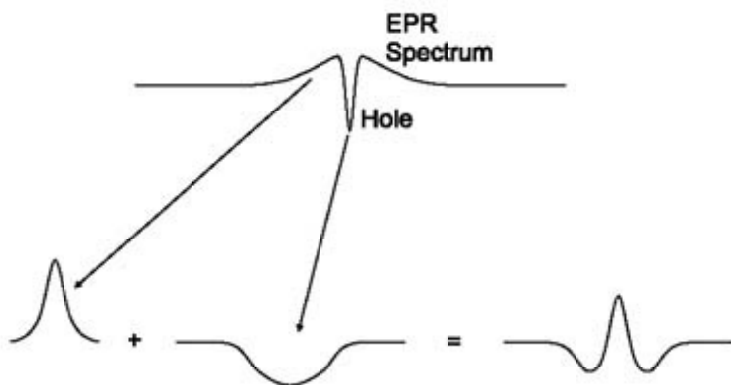


Figure 4.42: Echo shapes in a hole burning experiment.